electronic reprint

CRYSTALLOGRAPHIC COMMUNICATIONS

ISSN: 2056-9890
journals.iucr.org/e

fac-Triaqua(1,10-phenanthroline-κ^2N,N')(sulfato-κO)cobalt(II): crystal structure, Hirshfeld surface analysis and computational study

Zouaoui Setifi, Huey Chong Kwong, Edward R. T. Tiekink, Thierry Maris and Fatima Setifi

Acta Cryst. (2020). E**76**, 835–840

Acta Cryst E CRYSTALLOGRAPHIC COMMUNICATIONS

ISSN 2056-9890

fac-Triaqua(1,10-phenanthroline-κ^2N,N')(sulfato-κO)cobalt(II): crystal structure, Hirshfeld surface analysis and computational study

Zouaoui Setifi,[a,b]‡ Huey Chong Kwong,[c] Edward R. T. Tiekink,[c]* Thierry Maris[d] and Fatima Setifi[b]

[a]Département de Technologie, Faculté de Technologie, Université 20 Août 1955-Skikda, BP 26, Route d'El-Hadaiek, Skikda 21000, Algeria, [b]Laboratoire de Chimie, Ingénierie Moléculaire et Nanostructures (LCIMN), Université Ferhat Abbas Sétif 1, Sétif 19000, Algeria, [c]Research Centre for Crystalline Materials, School of Science and Technology, Sunway University, 47500 Bandar Sunway, Selangor Darul Ehsan, Malaysia, and [d]Department of Chemistry, Université de Montréal, 2900 Edouard-Montpetit Blvd, Montreal, Quebec, H3T1J4, Canada. *Correspondence e-mail: edwardt@sunway.edu.my

Received 6 May 2020
Accepted 8 May 2020

Edited by W. T. A. Harrison, University of Aberdeen, Scotland

‡ Additional correspondence author, e-mail: setifi_zouaoui@yahoo.fr.

Keywords: crystal structure; cobalt(II); hydrogen bonding; Hirshfeld surface analysis.

CCDC reference: 2002737

Supporting information: this article has supporting information at journals.iucr.org/e

The Co^{II} atom in the title complex, $[Co(SO_4)(C_{12}H_8N_2)(H_2O)_3]$ (or $C_{12}H_{14}CoN_2O_7S$), is octahedrally coordinated within a cis-N_2O_4 donor set defined by the chelating N-donors of the 1,10-phenanthroline ligand, sulfate-O and three aqua-O atoms, the latter occupying an octahedral face. In the crystal, supramolecular layers lying parallel to (110) are sustained by aqua-O—H···O(sulfate) hydrogen bonding. The layers stack along the *c*-axis direction with the closest directional interaction between them being a weak phenanthroline-C—H···O(sulfate) contact. There are four significant types of contact contributing to the calculated Hirshfeld surface: at 44.5%, the major contribution comes from O—H···O contacts followed by H···H (28.6%), H···C/C···H (19.5%) and C···C (5.7%) contacts. The dominance of the electrostatic potential force in the molecular packing is also evident in the calculated energy frameworks. The title complex is isostructural with its manganese, zinc and cadmium containing analogues and isomeric with its *mer*-triaqua analogue.

1. Chemical context

As a consequence of their ability to link metal ions in a variety of different ways, polynitrile anions, either functioning alone or in combination with neutral co-ligands, provide opportunities for the generation of molecular architectures with varying dimensions and topologies (Benmansour *et al.*, 2012). The presence of other potential donor groups such as those derived from –OH, –SH or $–NH_2$, together with their rigidity and electronic delocalization, mean that polynitrile anions can also lead to new magnetic and luminescent coordination polymers based on transition-metal ions (Benmansour *et al.*, 2010; Kayukov *et al.*, 2017; Lehchili *et al.*, 2017; Setifi *et al.*, 2017). Furthermore, the use of polynitrile anions for the synthesis of interesting discrete and polymeric bistable materials has been described (Setifi *et al.*, 2014; Milin *et al.*, 2016; Pittala *et al.*, 2017). In view of this coordinating ability, these ligands have also been explored for their utility in developing materials capable of magnetic exchange coupling (Addala *et al.*, 2015; Déniel *et al.*, 2017). It was during the course of attempts to prepare such complexes with 1,10-phenanthroline as a co-ligand that the title complex, (I), was unexpectedly

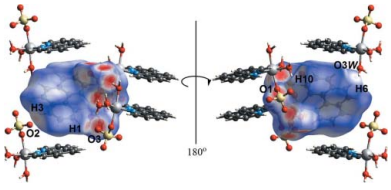

Table 1
Selected bond lengths (Å).

Co—O1	2.1386 (13)	Co—N2	2.1453 (16)
Co—O1*W*	2.1110 (14)	S1—O1	1.4997 (13)
Co—O2*W*	2.0782 (15)	S1—O2	1.4616 (14)
Co—O3*W*	2.1024 (14)	S1—O3	1.4813 (14)
Co—N1	2.1356 (15)	S1—O4	1.4784 (14)

obtained. Herein, the crystal and molecular structures of (I) are described, a study complemented by an analysis of the molecular packing by calculating the Hirshfeld surfaces as well as a computational chemistry study.

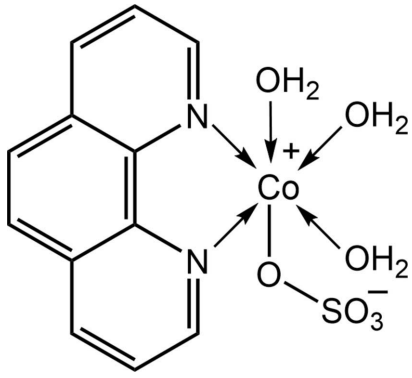

2. Structural commentary

The molecule of (I) is shown in Fig. 1 and selected geometric parameters are collated in Table 1. The Co^{II} complex features a chelating 1,10-phenanthroline ligand, a monodentate sulfate di-anion and three coordinated water molecules. The resulting N_2O_4 donor set defines a distorted octahedral coordination geometry for the Co^{II} atom, with the water molecules occupying one octahedral face. The greatest deviations from a regular geometry is seen in the restricted bite angle subtended by the 1,10-phenanthroline ligand, *i.e.* N1—Co1—N2 = 78.21 (6)°, and in the *trans* O2*W*—Co—N2 angle of 166.55 (6)°. The Co—N bond lengths are equal within

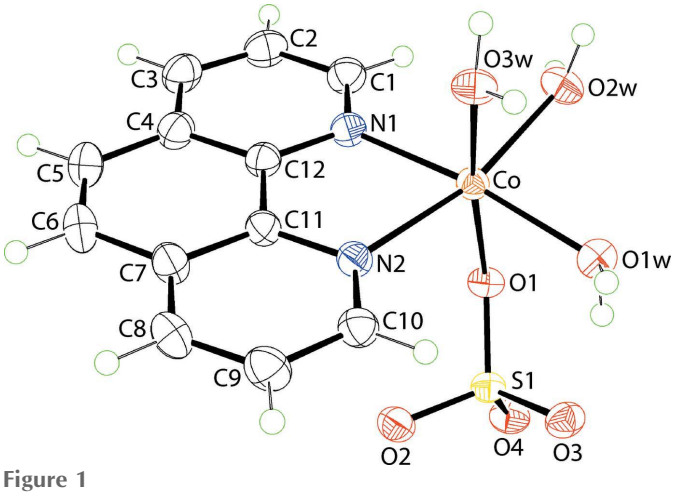

Figure 1
The molecular structure of (I) showing the atom-labelling scheme and displacement ellipsoids at the 50% probability level.

Table 2
Hydrogen-bond geometry (Å, °).

D—H···*A*	*D*—H	H···*A*	*D*···*A*	*D*—H···*A*
O1*W*—H1*W*···O3	0.84 (2)	1.89 (2)	2.680 (2)	158 (2)
O1*W*—H2*W*···O1^{i}	0.83 (1)	1.95 (1)	2.7818 (19)	172 (2)
O2*W*—H3*W*···O3^{ii}	0.84 (2)	1.91 (2)	2.744 (2)	175 (3)
O2*W*—H4*W*···O4^{iii}	0.85 (1)	1.93 (1)	2.770 (2)	167 (3)
O3*W*—H5*W*···O4^{i}	0.82 (2)	1.95 (2)	2.7548 (19)	168 (3)
O3*W*—H6*W*···O2^{iii}	0.82 (2)	1.84 (2)	2.6560 (19)	178 (3)
C3—H3···O2^{iv}	0.95	2.45	3.252 (3)	142

Symmetry codes: (i) $-x+1, y-\frac{1}{2}, -z+\frac{1}{2}$; (ii) $-x+1, y+\frac{1}{2}, -z+\frac{1}{2}$; (iii) $x+1, y, z$; (iv) $x+\frac{1}{2}, -y+\frac{3}{2}, -z+1$.

experimental error but the Co—O(aqua) bonds span an experimentally distinct range, Table 1. The observation that the shortest and longest Co—O(aqua) bonds have each aqua-O atom *trans* to a nitrogen atom suggests the differences in bond lengths are due to the considerable hydrogen bonding operating in the crystal. Indeed, there is an intramolecular aqua-O1*W*—H···O3(sulfate) hydrogen bond, Table 2. The coordinated sulfate-O1 atom forms the longer of the four sulfate-S—O bonds, Table 1. The S—O bond lengths formed by the non-coordinating sulfate-oxygen atoms spans an experimentally distinct range of 1.4616 (14) Å for S1—O2, to 1.4813 (14) Å for S1—O3. As discussed below, the sulfate-O1–O4 oxygen atoms form, respectively, one, one, two and two hydrogen bonds with the water molecules, which is consistent with the S1—O2 bond length being the shortest of the four bonds. The above notwithstanding, it is likely that the formal negative charge on the SO_3 residue is delocalized over the three non-coordinating S—O bonds.

3. Supramolecular features

Each of the aqua ligands donates two hydrogen bonds to different sulfate-O atoms, one of these hydrogen bonds is intramolecular while the remaining are intermolecular, Table 2. The result of the hydrogen bonding is the formation of a supramolecular layer lying parallel to (110). A simplified view of the hydrogen bonding scheme is shown in Fig. 2(*a*). The aqua molecule forming the intramolecular O1*W*—H···O3 hydrogen bond forms a second hydrogen bond to the coordinated O1 atom of a symmetry-related molecule, and the O2*W* aqua ligand of this molecule connects to the O3 atom of the original molecule, leading to the formation of a non-symmetric eight-membered {···HOH···O···HOCoO} synthon. The second hydrogen atom of the O2*W* ligand forms a connection to a sulfate-O4 atom, which is also hydrogen bonded to an O3*W* molecule, which forms an additional link to a symmetry related sulfate-O2 atom with the result a {···HOH···OSO···HOH···O} non-symmetric ten-membered synthon is formed. Two additional eight-membered synthons, {HOCoOH···OSO}, are formed as a result of the hydrogen-bonding scheme as adjacent pairs of aqua molecules effectively bridge two sulfoxide residues. As seen from Fig. 2(*b*), the 1,10-phenanthroline molecules project to either side of the supramolecular layer. The layers inter-digitate along [001],

Table 3
A summary of short interatomic contacts (Å) in (I)[a].

Contact	Distance	Symmetry operation
H2*W*···O1[b]	1.81	$-x+1, y-\frac{1}{2}, -z+\frac{1}{2}$
H3*W*···O3[b]	1.76	$-x+1, y+\frac{1}{2}, -z+\frac{1}{2}$
H4*W*···O4[b]	1.81	$x+1, y, z$
H5*W*···O4[b]	1.79	$-x+1, y-\frac{1}{2}, -z+\frac{1}{2}$
H6*W*···O2[b]	1.67	$x+1, y, z$
H1···O3	2.33	$-x+1, y+\frac{1}{2}, -z+\frac{1}{2}$
H3···O2	2.35	$x+\frac{1}{2}, -y+\frac{3}{2}, -z+1$
H6···O3*W*	2.51	$x-\frac{1}{2}, -y+\frac{1}{2}, -z+1$
H10···O1	2.40	$-x+1, y-\frac{1}{2}, -z+\frac{1}{2}$

Notes: (*a*) The interatomic distances are calculated in *Crystal Explorer 17* (Turner *et al.*, 2017) whereby the *X*—H bond lengths are adjusted to their neutron values; (*b*) these interactions correspond to conventional hydrogen bonds.

Fig. 2(*c*), with the closest connections between layers being phenanthroline-C—H···O2(sulfate) interactions, Table 2. A deeper analysis of the molecular packing is found in the next two sections of this paper.

4. Hirshfeld surface analysis

In order to understand further the interactions operating in the crystal of (I), the Hirshfeld surfaces and two-dimensional fingerprint plots were calculated employing the program *Crystal Explorer 17* (Turner *et al.*, 2017) and literature procedures (Tan *et al.*, 2019). The intermolecular O—H···O hydrogen bonds in (I), Table 2, are characterized as pairs of bright-red spots near the aqua-O and sulfate-O atoms on the Hirshfeld surface mapped over d_{norm} shown in Fig. 3. The faint-red spots near the phenanthroline-C—H (H1, H3 H6 and H10) atoms on the d_{norm}-mapped Hirshfeld surface in the two views of Fig. 4 represent the influence of the weak C3—H3···O2 and C10—H10···O1 interactions as well as H1···O3, H6···O3*W* short contacts, Table 3. The donors and acceptors of the weak C—H···O interaction are viewed as blue and red regions on the Hirshfeld surface mapped over the calculated electrostatic potential in Fig. 5, and which correspond to positive and negative electrostatic potentials.

The overall two-dimensional fingerprint plot of (I) is shown in Fig. 6(*a*). The overall contacts are also delineated into

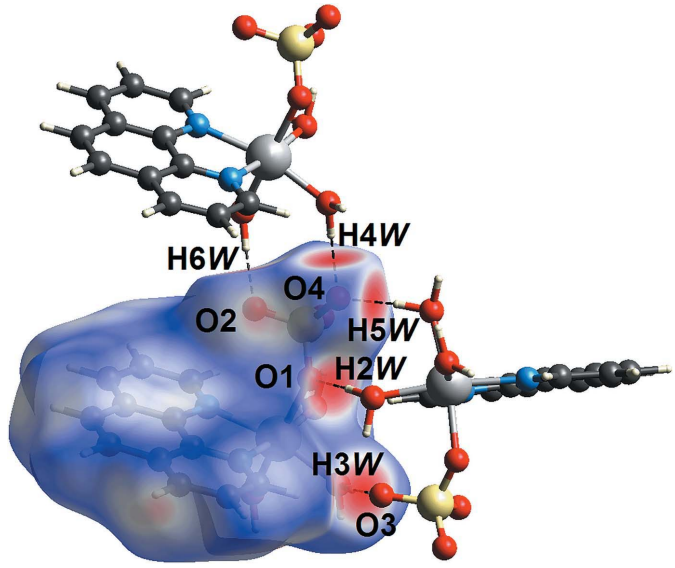

Figure 3
A view of the Hirshfeld surface mapped over d_{norm} for (I) in the range of −0.729 to +1.105 arbitrary units, highlighting O—H···O interactions.

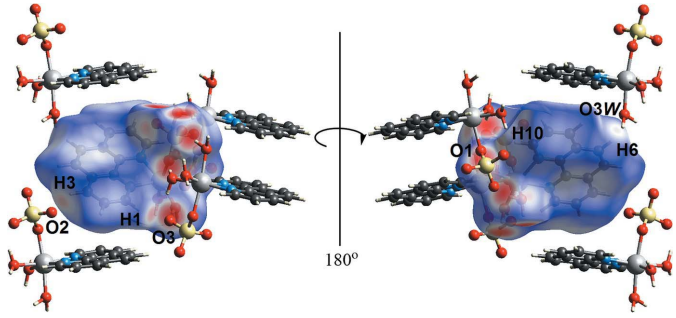

Figure 4
Two views of the Hirshfeld surface mapped over d_{norm} for (I) in the range of −0.729 to +1.105 arbitrary units, highlighting weak C—H···O interactions and short contacts.

H···H, H···O/O···H, H···C/C···H and C···C contacts, as displayed in Fig. 6(*b*)–(*e*), respectively. The short interatomic H···H contacts are characterized as the pair of beak-shaped

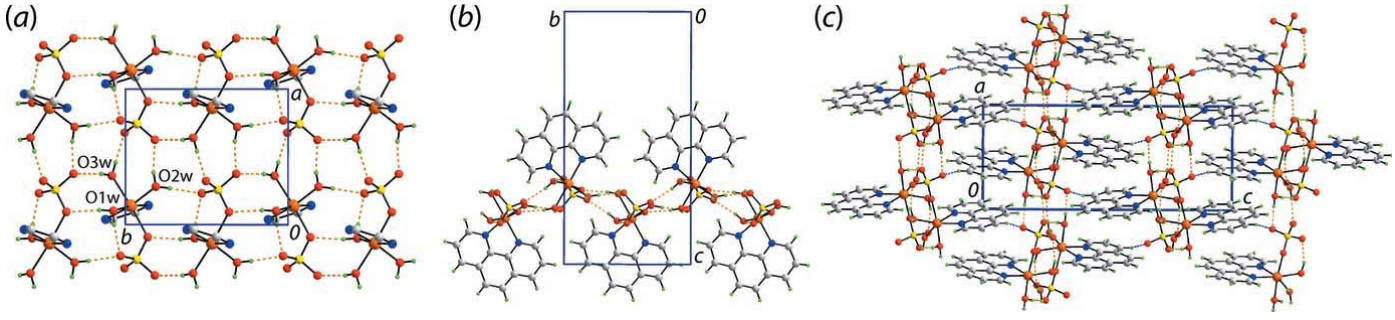

Figure 2
Molecular packing in the crystal of (I): (*a*) supramolecular layer sustained by aqua-O—H···O(sulfate) hydrogen bonding shown as orange dashed lines, only the five-membered chelate rings are shown for reasons of clarity, (*b*) a side-on view of the layer shown in (*a*) and (*c*) a view of the unit-cell contents down the *b* axis showing the stacking of layers along the *c*-axis direction, with the phenanthroline-C—H···O(sulfate) interactions between layers shown as blue dashed lines.

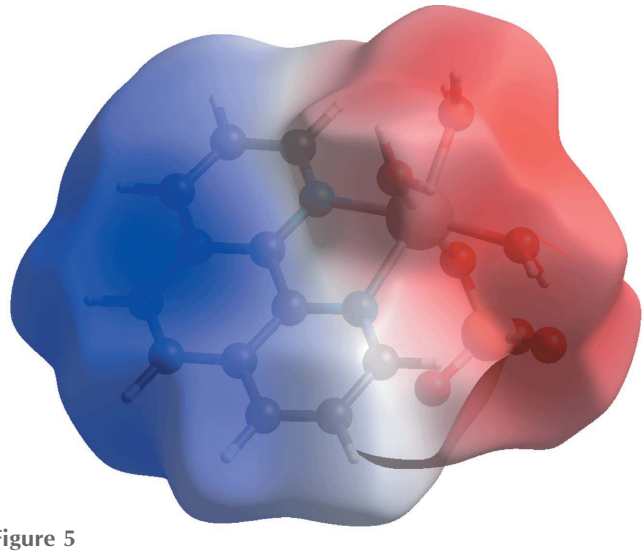

Figure 5
A view of the Hirshfeld surface mapped over the calculated electrostatic potential for (I). The potentials were calculated using the STO-3G basis set at Hartree–Fock level of theory over a range of −4.381 to 4.109 atomic units. The red and blue regions represent negative and positive electrostatic potentials, respectively.

tips at $d_e + d_i$ ∼2.3 Å, Fig. 6(*b*), and contribute 28.6% to the overall surface contacts. The significant O—H···O contacts between the aqua- and sulfate-O atoms make the major contribution to the overall contacts (44.5%), and these are represented as pairs of well-defined spikes at $d_e + d_i$ ∼1.7 Å in Fig. 6(*c*). The short interatomic H···C/C···H (19.5%) and C···C (5.7%) contacts are, respectively, characterized as pairs of broad symmetrical wings at $d_e + d_i$ ∼2.9 Å in Fig. 6(*d*), and the vase-shaped distribution of points at $d_e + d_i$ ∼3.5 Å in Fig. 6(*e*). The accumulated contribution of the remaining interatomic contacts is less than 2% and has a negligible effect on the packing.

5. Computational chemistry

In the present analysis, the pairwise interaction energies between the molecules in the crystal were calculated by summing up four different energy components, *i.e.* the electrostatic (E_{ele}), polarization (E_{pol}), dispersion (E_{dis}) and exchange-repulsion (E_{rep}) energy terms, after Turner *et al.* (2017). These energies were obtained by applying the wave functions calculated at the B3LYP/6-31G(d,p) level of theory. The benchmarked energies were scaled according to Mackenzie *et al.* (2017) while E_{ele}, E_{pol}, E_{dis} and E_{rep} were scaled as 1.057, 0.740, 0.871 and 0.618, respectively (Edwards *et al.*, 2017). The intermolecular interaction energies are collated in Table 4. Consistent with the presence of strong O—H···O hydrogen-bonding interactions in the crystal, the electrostatic energy component has a major influence in the formation of supramolecular architecture of (I), Table 4. The energy associated with the C—H···O interactions involving the sulfate-O atoms (−66.8 and −55.7 kJ mol^{-1}) are greater than for the C—H···O interaction involving the aqua-O atoms (−30.6 kJ mol^{-1}). The energy frameworks were also computed and illustrate the above conclusions, Fig. 7. These clearly demonstrate the dominance of the electrostatic potential energy in the molecular packing.

Table 4
A summary of interaction energies (kJ mol^{-1}) calculated for (I).

Contact	R (Å)	E_{ele}	E_{pol}	E_{dis}	E_{rep}	E_{tot}
O1*W*—H2*W*···O1^{i} + O3*W*—H5*W*···O4^{i} + O2*W*—H3*W*···O3^{ii} + C10—H10···O1^{i}	6.78	−330.8	−116.8	−49.6	180.1	−368.1
O3*W*—H6*W*···O2^{iii} + O2*W*—H4*W*···O4^{iii}	7.97	−198.3	−63.8	−16.4	121.0	−196.4
C5—H5···O3^{v} + C6—H6···O4^{v}	10.47	−46.2	−19.3	−9.8	7.8	−66.8
C3—H3···O2^{iv}	7.64	−17.3	−30.2	−42.3	35.3	−55.7
C6—H6···O3*W*^{vi}	8.03	−2.3	−13.7	−37.7	24.0	−30.6

Symmetry operations: (i) $-x+1, y-\frac{1}{2}, -z+\frac{1}{2}$; (ii) $-x+1, y+\frac{1}{2}, -z+\frac{1}{2}$; (iii) $x+1, y, z$; (iv) $x+\frac{1}{2}, -y+\frac{3}{2}, -z+1$; (v) $-x+\frac{1}{2}, -y+1, z+\frac{1}{2}$; (vi) $x-1/2, -y+\frac{1}{2}, -z+1$.

6. Database survey

There are several literature analogues of (I), *i.e.* molecules conforming to the general formula *fac*-*M*(1,10-phenanthroline)$(OH_2)_3OSO_3$. These include *M* = Mn (XATNAH; Zheng *et al.*, 2000), *M* = Zn (IJOQAA; Liu *et al.*, 2011) and *M* = Cd (RACWUO; Li *et al.*, 2003). The three literature structures are isostructural with (I). Literature analogues are also available for the isomeric *mer*-*M*(1,10-phenanthroline)$(OH_2)_3OSO_3$ species, *i.e.* *M* = Mn (UGOJUV; Zheng *et al.*, 2002), *M* = Fe (MIKJAS; Li *et al.*, 2007), *M* = Co (FICNOU; Li & Zhou, 1987) and *M* = Ni (ESUZOH; He *et al.*,

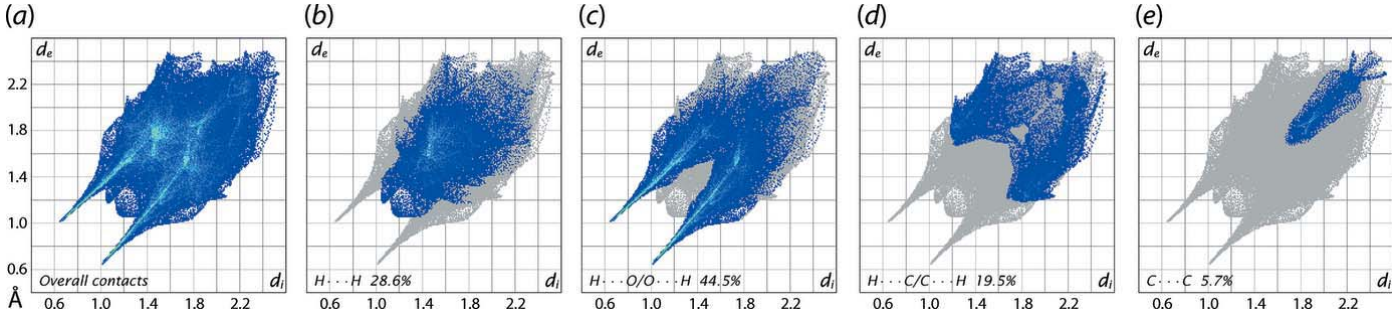

Figure 6
(*a*) The overall two-dimensional fingerprint plots for (I), and those delineated into (*b*) H···H, (*c*) O···H/H···O, (*d*) C···H/H···C and (*e*) C···C contacts.

Table 5
Percentage contributions to intermolecular contacts on the Hirshfeld surface calculated for (I).

Contact	Percentage contribution			
	(I), *M* = Co	IJOQAA, *M* = Zn	RACWUO, *M* = Cd	XATNAH, *M* = Mn
H···H	28.6	30.1	27.6	27.2
H···O/O···H	44.5	43.3	45.8	45.9
H···C/C···H	19.5	19.1	19.2	19.1
C···C	5.7	5.7	5.2	5.6
Others	1.7	1.8	2.2	2.2

2003). The four *mer*-isomers are also isostructural, crystallizing in the monoclinic space group $P2_1/c$. There are two pairs of structures (containing Mn and Co) crystallizing in both forms. For the Mn complexes, the authors reporting the structure of the *mer*-isomer indicated that both forms were formed concomitantly from the slow evaporation of a methanol solution of the complex (Zheng *et al.*, 2002). To a first approximation, the molecular packing in the *mer* form resembles that for the *fac*-isomer in that supramolecular layers are formed by hydrogen bonding whereby each aqua ligand hydrogen bonds to two different sulfate-O atoms, *i.e.* as for (I).

The key difference in the packing between the two isomers arises as one sulfate-O atom in the *mer*-isomer participates in three hydrogen bonds at the expense of the hydrogen bond involving the coordinated sulfate-O1 atom. The presence of inter-layer phenanthroline-C—H···O(sulfate) interactions persist as for the *fac*-isomer with the crucial difference that π–π stacking interactions are evident in the inter-layer region of the *mer*-form with the shortest separation being 3.76 Å.

The different packing arrangements result in different densities with that for (I) of 1.776 g cm^{-3} being greater than 1.723 g cm^{-3} for the *mer*-isomer (FICNOU; Li & Zhou, 1987). The calculated packing efficiencies follow this trend being 72.8 and 66.5%, respectively. Similar results are noted for the pair of Mn structures, *i.e.* 1.690 g cm^{-3} and 71.1% for the *fac*-isomer (Zheng *et al.*, 2000) *c.f.* 1.643 g cm^{-3} and 68.7% for the *mer*-isomer (Zheng *et al.*, 2000). The consistency of these parameters may suggest that the *fac*-isomer in these *M*(1,10-phenanthroline)$(OH_2)_3OSO_3$ complexes is the thermodynamically more stable form.

Given the isostructural relationship in the series (I), IJOQAA, RACWUO and XATNAH, it was thought of interest to compare the percentage contributions of the difference intermolecular contacts to the calculated Hirshfeld surfaces. Thus, these were calculated for the three literature structures as were the overall and delineated two-dimensional fingerprint plots. Qualitatively, the fingerprint plots had the same general appearance in accord with expectation (Jotani *et al.*, 2019). The calculated percentage contributions to the Hirshfeld surfaces for the four complexes are collated in Table 5. Clearly and as would be expected, the data in Table 5 reveal a high degree of concordance in the percentage contributions to the Hirshfeld surfaces between the four isostructural complexes.

7. Synthesis and crystallization

The title compound was synthesized solvothermally under autogenous pressure from a mixture of $CoSO_4{\cdot}7H_2O$ (28 mg, 0.1 mmol), 1,10-phenanthroline (18 mg, 0.1 mmol) and K(tcnoet) (45 mg, 0.2 mmol) in water–methanol (4:1*v*/*v*, 25 ml); where tcnoet is 1,1,3,3-tetracyano-2-ethoxypropenide. The mixture was sealed in a Teflon-lined autoclave and held at 403 K for 2 days, and then cooled to room temperature at a rate of 10 K h^{-1}; yield: 35%. Light-pink blocks of the title complex suitable for single-crystal X-ray diffraction were selected directly from the synthesized product.

8. Refinement

Crystal data, data collection and structure refinement details are summarized in Table 6. The carbon-bound H atoms were placed in calculated positions (C—H = 0.95 Å) and were included in the refinement in the riding-model approximation, with U_{iso}(H) set to 1.2U_{eq}(C). The oxygen-bound H atoms were located from a difference-Fourier map and refined with

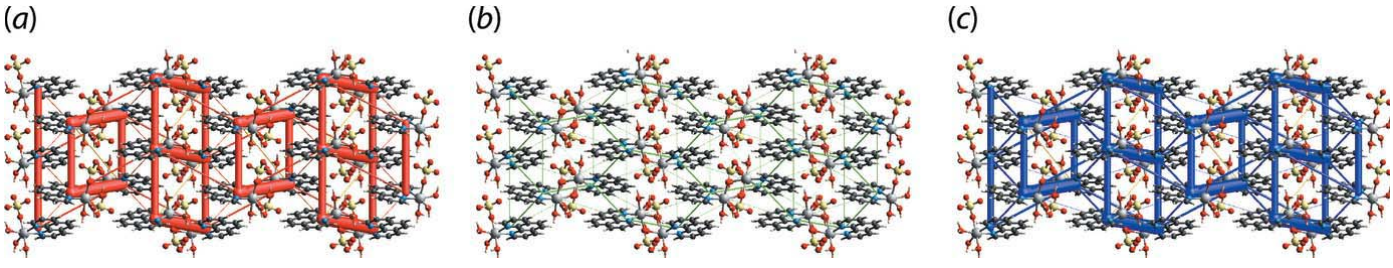

Figure 7
Perspective views of the energy frameworks calculated for (I), showing the (*a*) electrostatic potential force, (*b*) dispersion force and (*c*) total energy, each plotted down the *b* axis. The radii of the cylinders are proportional to the relative magnitudes of the corresponding energies and were adjusted to the same scale factor of 20 with a cut-off value of 5 kJ mol^{-1} within 2 × 2 × 2 unit cells.

O—H = 0.84±0.01 Å, and with U_{iso}(H) set to 1.5U_{eq}(O). Owing to poor agreement, four reflections, *i.e.* (0 1 4), (0 0 2), (0 1 2) and (0 0 4), were omitted from the final cycles of refinement. The absolute structure was determined based on differences in Friedel pairs included in the data set.

Funding information

FS gratefully acknowledges the Algerian Ministère de l'Enseignement Supérieur et de la Recherche Scientifique (MESRS), the Direction Générale de la Recherche Scientifique et du Développement Technologique (DG–RSDT) as well as the Université Ferhat Abbas Sétif 1 for financial support. The Canadian Foundation for Innovation is thanked for the support of the Metaljet instrument. Crystallographic research at Sunway University is supported by Sunway University Sdn Bhd (Grant no. STR-RCTR-RCCM-001-2019).

References

Addala, A., Setifi, F., Kottrup, K. G., Glidewell, C., Setifi, Z., Smith, G. & Reedijk, J. (2015). *Polyhedron*, **87**, 307–310.

Benmansour, S., Atmani, C., Setifi, F., Triki, S., Marchivie, M. & Gómez-García, C. J. (2010). *Coord. Chem. Rev.* **254**, 1468–1478.

Benmansour, S., Setifi, F., Triki, S. & Gómez-García, C. J. (2012). *Inorg. Chem.* **51**, 2359–2365.

Brandenburg, K. (2006). *DIAMOND*. Crystal Impact GbR, Bonn, Germany.

Bruker (2013). *APEX2* and *SAINT*. Bruker AXS Inc., Madison, Wisconsin, USA.

Bruker (2016). *SADABS*. Bruker AXS Inc., Madison, Wisconsin, USA.

Déniel, K., Cosquer, N., Conan, F., Triki, S. & Gómez-García, C. J. (2017). *Polyhedron*, **125**, 50–56.

Edwards, A. J., Mackenzie, C. F., Spackman, P. R., Jayatilaka, D. & Spackman, M. A. (2017). *Faraday Discuss.* **203**, 93–112.

Farrugia, L. J. (2012). *J. Appl. Cryst.* **45**, 849–854.

He, H.-Y., Zhou, Y.-L. & Zhu, L.-G. (2003). *Z. Kristallogr. New Cryst. Struct.* **218**, 563–564.

Jotani, M. M., Wardell, J. L. & Tiekink, E. R. T. (2019). *Z. Kristallogr. Cryst. Mater.* **234**, 43–57.

Kayukov, Y. S., Karpov, S. V., Grigor'ev, A. A., Nasakin, O. E., Tafeenko, V. A., Lyssenko, K. A., Shapovalov, A. V. & Varaksina, E. A. (2017). *Dalton Trans.* **46**, 16925–16938.

Lehchili, F., Setifi, F., Liu, X., Saneei, A., Kučeráková, M., Setifi, Z., Dušek, M., Poupon, M., Pourayoubi, M. & Reedijk, J. (2017). *Polyhedron*, **131**, 27–33.

Li, J. M. & Zhou, K. J. (1987). *Chin. J. Struct. Chem.* **6**, 198–200.

Li, P.-Z., Lu, X.-M., Liu, B., Wang, S. & Wang, X.-J. (2007). *Inorg. Chem.* **46**, 5823–5825.

Li, X., Cao, R., Bi, W., Sun, D. & Hong, M. (2003). *Acta Cryst.* E**59**, m230–m231.

Liu, H., Qin, H., Zhang, Y.-J., Yang, H.-W. & Zhang, J. (2011). *Acta Cryst.* E**67**, m280–m281.

Mackenzie, C. F., Spackman, P. R., Jayatilaka, D. & Spackman, M. A. (2017). *IUCrJ*, **4**, 575–587.

Milin, E., Belaïd, S., Patinec, V., Triki, S., Chastanet, G. & Marchivie, M. (2016). *Inorg. Chem.* **55**, 9038–9046.

Table 6
Experimental details.

Crystal data	
Chemical formula	$[Co(SO_4)(C_{12}H_8N_2)(H_2O)_3]$
M_r	389.24
Crystal system, space group	Orthorhombic, $P2_12_12_1$
Temperature (K)	150
a, b, c (Å)	7.9732 (4), 9.5589 (4), 19.0955 (9)
V (Å^3)	1455.36 (12)
Z	4
Radiation type	Ga $K\alpha$, λ = 1.34139 Å
μ (mm^{-1})	7.61
Crystal size (mm)	0.08 × 0.08 × 0.05
Data collection	
Diffractometer	Bruker Venture Metaljet
Absorption correction	Multi-scan (*SADABS*; Bruker, 2016)
T_{min}, T_{max}	0.064, 0.155
No. of measured, independent and observed [$I > 2\sigma(I)$] reflections	25223, 3202, 3126
R_{int}	0.033
(sin $\theta/\lambda)_{max}$ (Å^{-1})	0.650
Refinement	
$R[F^2 > 2\sigma(F^2)]$, $wR(F^2)$, S	0.017, 0.046, 0.99
No. of reflections	3202
No. of parameters	227
No. of restraints	6
H-atom treatment	H atoms treated by a mixture of independent and constrained refinement
$\Delta\rho_{max}$, $\Delta\rho_{min}$ (e Å^{-3})	0.51, −0.58
Absolute structure	Flack x determined using 1194 quotients $[(I^+)-(I^-)]/[(I^+)+(I^-)]$ (Parsons *et al.*, 2013).
Absolute structure parameter	0.0101 (17)

Computer programs: *APEX2* and *SAINT* (Bruker, 2013), *SHELXS* (Sheldrick, 2015*a*), *SHELXL2018/3* (Sheldrick, 2015*b*), *ORTEP-3 for Windows* (Farrugia, 2012), *DIAMOND* (Brandenburg, 2006) and *publCIF* (Westrip, 2010).

Parsons, S., Flack, H. D. & Wagner, T. (2013). *Acta Cryst.* B**69**, 249–259.

Pittala, N., Thétiot, F., Charles, C., Triki, S., Boukheddaden, K., Chastanet, G. & Marchivie, M. (2017). *Chem. Commun.* **53**, 8356–8359.

Setifi, F., Konieczny, P., Glidewell, C., Arefian, M., Pelka, R., Setifi, Z. & Mirzaei, M. (2017). *J. Mol. Struct.* **1149**, 149–154.

Setifi, F., Milin, E., Charles, C., Thétiot, F., Triki, S. & Gómez-García, C. J. (2014). *Inorg. Chem.* **53**, 97–104.

Sheldrick, G. M. (2015*a*). *Acta Cryst.* A**71**, 3–8.

Sheldrick, G. M. (2015*b*). *Acta Cryst.* C**71**, 3–8.

Tan, S. L., Jotani, M. M. & Tiekink, E. R. T. (2019). *Acta Cryst.* E**75**, 308–318.

Turner, M. J., Mckinnon, J. J., Wolff, S. K., Grimwood, D. J., Spackman, P. R., Jayatilaka, D. & Spackman, M. A. (2017). *Crystal Explorer 17*. The University of Western Australia.

Westrip, S. P. (2010). *J. Appl. Cryst.* **43**, 920–925.

Zheng, Y.-Q., Lin, J.-L. & Kong, Z.-P. (2000). *Z. Kristallogr. New Cryst. Struct.* **215**, 531–532.

Zheng, Y.-Q., Sun, J. & Lin, J.-L. (2002). *Z. Kristallogr. New Cryst. Struct.* **217**, 189–191.

supporting information

Acta Cryst. (2020). E**76**, 835-840 [https://doi.org/10.1107/S2056989020006271]

fac-Triaqua(1,10-phenanthroline-κ^2N,N')(sulfato-κO)cobalt(II): crystal structure, Hirshfeld surface analysis and computational study

Zouaoui Setifi, Huey Chong Kwong, Edward R. T. Tiekink, Thierry Maris and Fatima Setifi

Computing details

Data collection: *APEX2* (Bruker, 2013); cell refinement: *SAINT* (Bruker, 2013); data reduction: *SAINT* (Bruker, 2013); program(s) used to solve structure: *SHELXS* (Sheldrick, 2015*a*); program(s) used to refine structure: *SHELXL2018/3* (Sheldrick, 2015*b*); molecular graphics: *ORTEP-3 for Windows* (Farrugia, 2012), *DIAMOND* (Brandenburg, 2006); software used to prepare material for publication: *publCIF* (Westrip, 2010).

fac-Triaqua(1,10-phenanthroline-κ^2N,N')(sulfato-κO)cobalt(II)

Crystal data

$[Co(SO_4)(C_{12}H_8N_2)(H_2O)_3]$
M_r = 389.24
Orthorhombic, $P2_12_12_1$
a = 7.9732 (4) Å
b = 9.5589 (4) Å
c = 19.0955 (9) Å
V = 1455.36 (12) Å^3
Z = 4
$F(000)$ = 796
D_x = 1.776 Mg m^{-3}
Ga $K\alpha$ radiation, λ = 1.34139 Å
Cell parameters from 9840 reflections
θ = 4.0–60.7°
μ = 7.61 mm^{-1}
T = 150 K
Prism, light-pink
0.08 × 0.08 × 0.05 mm

Data collection

Bruker Venture Metaljet diffractometer
Radiation source: Metal Jet, Gallium Liquid Metal Jet Source
Helios MX Mirror Optics monochromator
Detector resolution: 10.24 pixels mm^{-1}
ω and φ scans
Absorption correction: multi-scan (SADABS; Bruker, 2016)
T_{min} = 0.064, T_{max} = 0.155
25223 measured reflections
3202 independent reflections
3126 reflections with $I > 2\sigma(I)$
R_{int} = 0.033
θ_{max} = 60.6°, θ_{min} = 4.5°
h = −10→10
k = −12→12
l = −24→24

Refinement

Refinement on F^2
Least-squares matrix: full
$R[F^2 > 2\sigma(F^2)]$ = 0.017
$wR(F^2)$ = 0.046
S = 0.99
3202 reflections
227 parameters
6 restraints
Primary atom site location: structure-invariant direct methods
Secondary atom site location: difference Fourier map
Hydrogen site location: mixed
H atoms treated by a mixture of independent and constrained refinement
$w = 1/[\sigma^2(F_o^2) + (0.0202P)^2]$ where $P = (F_o^2 + 2F_c^2)/3$
$(\Delta/\sigma)_{max}$ = 0.001
$\Delta\rho_{max}$ = 0.51 e Å^{-3}
$\Delta\rho_{min}$ = −0.58 e Å^{-3}

Extinction correction: SHELXL-2018/3 (Sheldrick, 2015*b*), $Fc^{*}=kFc[1+0.001xFc^{2}\lambda^{3}/\sin(2\theta)]^{-1/4}$
Extinction coefficient: 0.0057 (5)

Absolute structure: Flack *x* determined using 1194 quotients $[(I^{+})-(I)]/[(I^{+})+(I)]$ (Parsons *et al.*, 2013).
Absolute structure parameter: 0.0101 (17)

Special details

Geometry. All esds (except the esd in the dihedral angle between two l.s. planes) are estimated using the full covariance matrix. The cell esds are taken into account individually in the estimation of esds in distances, angles and torsion angles; correlations between esds in cell parameters are only used when they are defined by crystal symmetry. An approximate (isotropic) treatment of cell esds is used for estimating esds involving l.s. planes.

Fractional atomic coordinates and isotropic or equivalent isotropic displacement parameters (Å²)

	x	*y*	*z*	U_{iso}*/U_{eq}
Co	0.63811 (3)	0.53373 (3)	0.31720 (2)	0.02111 (9)
S1	0.24258 (5)	0.56910 (4)	0.27630 (2)	0.02212 (11)
O1	0.40704 (16)	0.63702 (14)	0.29351 (7)	0.0239 (3)
O2	0.17822 (17)	0.49545 (15)	0.33775 (7)	0.0291 (3)
O3	0.26932 (17)	0.46986 (15)	0.21777 (7)	0.0289 (3)
O4	0.12543 (18)	0.68089 (14)	0.25463 (7)	0.0290 (3)
O1W	0.60122 (18)	0.42633 (14)	0.22184 (7)	0.0267 (3)
H1W	0.5005 (18)	0.431 (3)	0.2097 (13)	0.040*
H2W	0.607 (3)	0.3405 (14)	0.2144 (14)	0.040*
O2W	0.77952 (18)	0.68717 (15)	0.26762 (8)	0.0296 (3)
H3W	0.768 (4)	0.7735 (15)	0.2743 (14)	0.044*
H4W	0.8839 (17)	0.673 (3)	0.2607 (15)	0.044*
O3W	0.85965 (17)	0.41650 (15)	0.32821 (7)	0.0281 (3)
H5W	0.874 (4)	0.353 (2)	0.2999 (12)	0.042*
H6W	0.9583 (19)	0.440 (3)	0.3324 (14)	0.042*
N1	0.6414 (2)	0.64091 (16)	0.41532 (8)	0.0252 (3)
N2	0.5377 (2)	0.37822 (16)	0.38651 (8)	0.0240 (3)
C1	0.6826 (3)	0.7733 (2)	0.42840 (11)	0.0307 (4)
H1	0.716162	0.831005	0.390391	0.037*
C2	0.6788 (3)	0.8312 (2)	0.49569 (12)	0.0349 (5)
H2	0.706310	0.926898	0.502638	0.042*
C3	0.6351 (3)	0.7487 (2)	0.55149 (12)	0.0357 (5)
H3	0.634774	0.786001	0.597609	0.043*
C4	0.5906 (3)	0.6081 (2)	0.53970 (11)	0.0311 (4)
C5	0.5383 (3)	0.5154 (3)	0.59456 (11)	0.0374 (5)
H5	0.537335	0.547683	0.641615	0.045*
C6	0.4904 (3)	0.3828 (3)	0.58034 (11)	0.0394 (5)
H6	0.456658	0.323326	0.617613	0.047*
C7	0.4897 (3)	0.3302 (2)	0.50992 (11)	0.0315 (4)
C8	0.4422 (3)	0.1926 (2)	0.49259 (12)	0.0358 (5)
H8	0.410012	0.128509	0.528178	0.043*
C9	0.4430 (3)	0.1523 (2)	0.42371 (12)	0.0350 (5)
H9	0.411464	0.059775	0.411121	0.042*
C10	0.4904 (3)	0.2480 (2)	0.37212 (11)	0.0290 (4)
H10	0.488688	0.218795	0.324580	0.035*

C11	0.5388 (2)	0.4191 (2)	0.45479 (10)	0.0251 (4)
C12	0.5919 (2)	0.5600 (2)	0.46986 (10)	0.0258 (4)

Atomic displacement parameters (Å²)

	U^{11}	U^{22}	U^{33}	U^{12}	U^{13}	U^{23}
Co	0.02084 (13)	0.02088 (13)	0.02160 (13)	−0.00016 (10)	0.00033 (10)	0.00127 (10)
S1	0.0203 (2)	0.0203 (2)	0.0258 (2)	−0.00016 (15)	−0.00058 (17)	−0.00105 (15)
O1	0.0203 (6)	0.0225 (6)	0.0291 (6)	−0.0006 (5)	−0.0005 (5)	−0.0017 (5)
O2	0.0262 (6)	0.0301 (7)	0.0311 (7)	−0.0029 (6)	0.0008 (5)	0.0037 (5)
O3	0.0282 (6)	0.0279 (6)	0.0306 (7)	−0.0006 (6)	−0.0015 (6)	−0.0074 (6)
O4	0.0235 (6)	0.0256 (6)	0.0378 (7)	0.0016 (6)	−0.0023 (6)	0.0027 (5)
O1W	0.0273 (7)	0.0240 (6)	0.0287 (7)	0.0042 (5)	−0.0013 (6)	−0.0016 (5)
O2W	0.0244 (7)	0.0244 (6)	0.0399 (8)	0.0008 (6)	0.0046 (6)	0.0047 (6)
O3W	0.0221 (6)	0.0250 (6)	0.0371 (7)	0.0012 (6)	−0.0018 (6)	−0.0011 (5)
N1	0.0242 (7)	0.0253 (7)	0.0259 (7)	0.0006 (7)	−0.0010 (7)	0.0000 (6)
N2	0.0225 (7)	0.0251 (8)	0.0242 (7)	−0.0003 (6)	0.0009 (6)	0.0010 (6)
C1	0.0318 (11)	0.0275 (9)	0.0329 (10)	−0.0025 (8)	−0.0020 (8)	−0.0001 (8)
C2	0.0354 (11)	0.0292 (10)	0.0402 (11)	−0.0022 (9)	−0.0043 (9)	−0.0074 (8)
C3	0.0365 (11)	0.0404 (11)	0.0302 (10)	−0.0001 (10)	−0.0014 (10)	−0.0109 (8)
C4	0.0296 (10)	0.0363 (10)	0.0273 (9)	0.0006 (8)	−0.0011 (8)	−0.0032 (8)
C5	0.0423 (12)	0.0468 (12)	0.0231 (9)	−0.0016 (10)	0.0031 (8)	−0.0016 (9)
C6	0.0461 (13)	0.0474 (13)	0.0247 (10)	−0.0035 (11)	0.0058 (10)	0.0064 (9)
C7	0.0314 (10)	0.0347 (10)	0.0286 (9)	−0.0023 (9)	0.0038 (8)	0.0045 (8)
C8	0.0386 (12)	0.0341 (11)	0.0348 (11)	−0.0053 (10)	0.0064 (9)	0.0084 (9)
C9	0.0381 (11)	0.0270 (9)	0.0400 (11)	−0.0056 (9)	0.0029 (9)	0.0024 (9)
C10	0.0289 (10)	0.0288 (9)	0.0293 (10)	−0.0023 (8)	0.0015 (8)	−0.0021 (8)
C11	0.0234 (8)	0.0277 (9)	0.0244 (8)	0.0003 (7)	0.0011 (7)	0.0008 (7)
C12	0.0236 (8)	0.0285 (9)	0.0253 (9)	0.0011 (7)	−0.0005 (7)	−0.0006 (7)

Geometric parameters (Å, º)

Co—O1	2.1386 (13)	C1—C2	1.399 (3)
Co—O1W	2.1110 (14)	C1—H1	0.9500
Co—O2W	2.0782 (15)	C2—C3	1.371 (3)
Co—O3W	2.1024 (14)	C2—H2	0.9500
Co—N1	2.1356 (15)	C3—C4	1.408 (3)
Co—N2	2.1453 (16)	C3—H3	0.9500
S1—O1	1.4997 (13)	C4—C12	1.411 (3)
S1—O2	1.4616 (14)	C4—C5	1.434 (3)
S1—O3	1.4813 (14)	C5—C6	1.351 (4)
S1—O4	1.4784 (14)	C5—H5	0.9500
O1W—H1W	0.837 (12)	C6—C7	1.436 (3)
O1W—H2W	0.834 (13)	C6—H6	0.9500
O2W—H3W	0.840 (13)	C7—C11	1.409 (3)
O2W—H4W	0.853 (12)	C7—C8	1.408 (3)
O3W—H5W	0.822 (12)	C8—C9	1.371 (3)
O3W—H6W	0.822 (13)	C8—H8	0.9500

N1—C1	1.331 (3)	C9—C10	1.397 (3)
N1—C12	1.356 (2)	C9—H9	0.9500
N2—C10	1.329 (3)	C10—H10	0.9500
N2—C11	1.361 (2)	C11—C12	1.441 (3)

O2W—Co—O3W	88.05 (6)	N1—C1—C2	122.9 (2)
O2W—Co—O1W	91.48 (6)	N1—C1—H1	118.6
O3W—Co—O1W	86.80 (6)	C2—C1—H1	118.6
O2W—Co—N1	93.13 (6)	C3—C2—C1	119.5 (2)
O3W—Co—N1	99.08 (6)	C3—C2—H2	120.3
O2W—Co—O1	92.59 (6)	C1—C2—H2	120.3
O1—Co—O3W	172.31 (5)	C2—C3—C4	119.26 (19)
O1W—Co—O1	85.53 (5)	C2—C3—H3	120.4
N1—Co—O1	88.54 (6)	C4—C3—H3	120.4
O1W—Co—N1	172.65 (6)	C3—C4—C12	117.42 (19)
O2W—Co—N2	166.55 (6)	C3—C4—C5	123.1 (2)
O3W—Co—N2	83.25 (6)	C12—C4—C5	119.4 (2)
O1W—Co—N2	98.23 (6)	C6—C5—C4	121.0 (2)
N1—Co—N2	78.21 (6)	C6—C5—H5	119.5
O1—Co—N2	97.41 (6)	C4—C5—H5	119.5
O2—S1—O4	110.56 (8)	C5—C6—C7	121.2 (2)
O2—S1—O3	110.35 (8)	C5—C6—H6	119.4
O4—S1—O3	110.04 (8)	C7—C6—H6	119.4
O2—S1—O1	109.85 (8)	C11—C7—C8	117.58 (19)
O4—S1—O1	107.51 (8)	C11—C7—C6	119.2 (2)
O3—S1—O1	108.47 (8)	C8—C7—C6	123.3 (2)
S1—O1—Co	126.85 (8)	C9—C8—C7	119.13 (19)
Co—O1W—H1W	110.3 (18)	C9—C8—H8	120.4
Co—O1W—H2W	128.2 (19)	C7—C8—H8	120.4
H1W—O1W—H2W	93 (3)	C8—C9—C10	119.6 (2)
Co—O2W—H3W	125 (2)	C8—C9—H9	120.2
Co—O2W—H4W	119 (2)	C10—C9—H9	120.2
H3W—O2W—H4W	106 (3)	N2—C10—C9	123.01 (19)
Co—O3W—H5W	117 (2)	N2—C10—H10	118.5
Co—O3W—H6W	132 (2)	C9—C10—H10	118.5
H5W—O3W—H6W	97 (3)	N2—C11—C7	122.72 (18)
C1—N1—C12	118.04 (17)	N2—C11—C12	117.50 (16)
C1—N1—Co	128.58 (14)	C7—C11—C12	119.78 (18)
C12—N1—Co	113.38 (12)	N1—C12—C4	122.85 (18)
C10—N2—C11	117.96 (16)	N1—C12—C11	117.73 (16)
C10—N2—Co	128.85 (14)	C4—C12—C11	119.43 (18)
C11—N2—Co	112.92 (12)		

O2—S1—O1—Co	67.05 (11)	C10—N2—C11—C7	−1.0 (3)
O4—S1—O1—Co	−172.59 (9)	Co—N2—C11—C7	−175.48 (16)
O3—S1—O1—Co	−53.64 (11)	C10—N2—C11—C12	179.40 (17)
C12—N1—C1—C2	0.7 (3)	Co—N2—C11—C12	4.9 (2)
Co—N1—C1—C2	179.75 (16)	C8—C7—C11—N2	1.7 (3)

N1—C1—C2—C3	1.7 (3)	C6—C7—C11—N2	−178.4 (2)
C1—C2—C3—C4	−1.6 (3)	C8—C7—C11—C12	−178.70 (19)
C2—C3—C4—C12	−0.7 (3)	C6—C7—C11—C12	1.2 (3)
C2—C3—C4—C5	−178.1 (2)	C1—N1—C12—C4	−3.3 (3)
C3—C4—C5—C6	177.4 (2)	Co—N1—C12—C4	177.58 (15)
C12—C4—C5—C6	0.0 (4)	C1—N1—C12—C11	176.72 (17)
C4—C5—C6—C7	−0.2 (4)	Co—N1—C12—C11	−2.4 (2)
C5—C6—C7—C11	−0.4 (4)	C3—C4—C12—N1	3.2 (3)
C5—C6—C7—C8	179.5 (2)	C5—C4—C12—N1	−179.3 (2)
C11—C7—C8—C9	−1.1 (3)	C3—C4—C12—C11	−176.74 (19)
C6—C7—C8—C9	179.0 (2)	C5—C4—C12—C11	0.8 (3)
C7—C8—C9—C10	−0.1 (4)	N2—C11—C12—N1	−1.7 (3)
C11—N2—C10—C9	−0.3 (3)	C7—C11—C12—N1	178.67 (18)
Co—N2—C10—C9	173.15 (16)	N2—C11—C12—C4	178.26 (17)
C8—C9—C10—N2	0.9 (4)	C7—C11—C12—C4	−1.4 (3)

Hydrogen-bond geometry (Å, º)

D—H···*A*	*D*—H	H···*A*	*D*···*A*	*D*—H···*A*
O1*W*—H1*W*···O3	0.84 (2)	1.89 (2)	2.680 (2)	158 (2)
O1*W*—H2*W*···O1^{i}	0.83 (1)	1.95 (1)	2.7818 (19)	172 (2)
O2*W*—H3*W*···O3^{ii}	0.84 (2)	1.91 (2)	2.744 (2)	175 (3)
O2*W*—H4*W*···O4^{iii}	0.85 (1)	1.93 (1)	2.770 (2)	167 (3)
O3*W*—H5*W*···O4^{i}	0.82 (2)	1.95 (2)	2.7548 (19)	168 (3)
O3*W*—H6*W*···O2^{iii}	0.82 (2)	1.84 (2)	2.6560 (19)	178 (3)
C3—H3···O2^{iv}	0.95	2.45	3.252 (3)	142

Symmetry codes: (i) −*x*+1, *y*−1/2, −*z*+1/2; (ii) −*x*+1, *y*+1/2, −*z*+1/2; (iii) *x*+1, *y*, *z*; (iv) *x*+1/2, −*y*+3/2, −*z*+1.